In-process detection of fiber cutting in low consistency refining based on measurement of forces on refiner bars

R. HARIRFOROUSH, J. OLSON, AND P. WILD

ABSTRACT: A major drawback of low consistency refining is the degradation of mechanical properties due to fiber cutting at high refining energies. Conventional strategies to avoid fiber cutting are based on post-refining measurement of pulp properties and, typically, this does not enable rapid adjustment of refiner operation in response to the onset of fiber cutting. The objective of this study is to detect the onset of fiber cutting by using custom-designed piezoelectric force sensors that measure shear and normal forces applied to pulp fibers by the refiner bars. Trials are performed in an AIKAWA/Advanced Fiber Technologies Inc. 16-in. single-disc low consistency refiner. The trials are run using mechanical softwood SPF (spruce, pine, and fir) pulp with 378 ml CSF at 2.5% and 3.5% consistency at rotational speeds of 800 rpm, 1000 rpm, and 1200 rpm. Distributions of the peak normal and shear forces and peak coefficient of friction are determined for each operating condition, and a two-parameter Weibull function is fit to each of these distributions. The scale parameter, which is one of the key parameters of the Weibull function, is calculated, and length-weighted fiber length is plotted as a function of this parameter. The results show that the onset of fiber cutting consistently corresponds to a distinct transition in the plot of length-weighted fiber length versus scale parameter. This transition is believed to be caused by a fundamental transition in the fiber-bar interaction. Moreover, frequency analysis of the sensor data shows that the magnitude of the dominant frequency remains relatively constant while the plate gap is reduced, up to a threshold value, which corresponds to the onset of fiber cutting. These results suggest that these sensors have potential to be used for in-process detection of the onset of fiber cutting.

Application: The application of this study is in-process detection of fiber cutting in low-consistency mechanical refining.

Mechanical pulping is an energy intensive process. For example, in British Columbia (BC), 78 refiners consume 5400 GWh/yr or 11% of BC's total electrical energy production [1], and the bulk of this energy is consumed in the mechanical pulping process. With the increasing cost of energy, the long-term survival of mechanical pulping may depend on reducing energy consumption of this process.

One method of diminishing energy consumption in mechanical pulping is to decrease the number of refining treatments at high consistency (HC) and increase the number of treatments at low consistency (LC). LC refining of mechanical pulp has been shown to be more energy efficient than conventional HC refining [2-5]. Moreover, LC refining is effective for removal of shives, external fibrillation of fibers, removal of latency, and improving fiber networking and bonding capabilities [6,7]. However, the degradation of mechanical properties due to fiber cutting at high refining energies has limited the widespread adoption of LC refining [1]. Understanding the relation between refiner operating conditions and resulting pulp properties is essential to reduce fiber cutting.

In mechanical refining, as the plate gap is closed, fibers are subjected to increasing compressive and shear forces that lead to an increase in net refiner power. Based on pilot and mill-scale LC refining studies, Luukkonen et al. found that the plate gap is a key link between the refiner process variables and resulting changes in pulp properties [1]. In a separate study, Luukkonen et al. [8] proposed a methodology to correlate operating conditions to pulp quality by relating the refiner operating conditions (i.e., power, flow rate, rotational speed, and plate gap) to fiber quality (i.e., fiber length and freeness) and then relating fiber quality to pulp handsheet quality (i.e., tensile, tear, and bulk). They also showed that pulp quality remains constant as the gap is closed, until a critical gap, which is characterized by the onset of significant fiber cutting, is reached. Beyond the critical gap, fiber cutting commences and paper strength is reduced. Moreover, beyond this point, the relationship between refining power and plate gap deviates from linearity [9].

Similar results were observed by Nugroho [10] for various mixes of softwood and hardwood chemical pulps in LC refining. Refining power increased as the plate gap decreased and, at a critical gap between 0.3 to 0.5 mm, the power sharply increased. Moreover, the fiber length and freeness decreased when the plate gap reached the critical gap. This transition occurred for all of the trial conditions.

Elahimehr et al. [11] studied the relationship between fiber length and plate gap in a AIKAWA 16-in. pilot-scale LC refiner. Trials were run at three rotational speeds, with four refiner plate patterns, and at 3% consistency. They found that mean fiber length was unchanged until the plate gap reached a critical gap, near 0.25 mm. The mean fiber length significantly decreased for the plate gaps smaller than the critical gap. Results also showed that increasing the rotational speed increases the critical gap.

Berg et al. [12] found that power increases linearly as the plate gap is reduced over the range of 0.1–0.2 mm in a two-zone TwinFlo72 LC refiner. They calculated average forces applied to fibers using the expression developed by Kerekes [13]. Fiber cutting was defined as the point where the ratio of outlet to inlet fiber length was equal to 0.95. Plate gap, forces on fibers, and specific edge load (SEL), defined as the energy expended per unit refiner bar length over one bar-crossing event, were found to predict fiber cutting.

In all of the studies previously discussed here, fiber cutting is detected by post-refining measurement of pulp properties. Typically, this approach does not enable rapid in-process adjustment of refiner operation in response to the onset of fiber cutting. These studies also do not address the mechanical interactions between fibers and refiner bars. Kerekes [14] suggests that bar force (i.e., the force applied to pulp fibers by the refiner bars) is the key parameter between bars and fibers in refining that cause important changes in fiber properties.

A piezoelectric sensor has been developed to measure bar forces. The sensor uses the piezoelectric effect, which is the ability of certain materials to generate an electric charge in response to applied mechanical stress. This sensor, referred to here as the refiner force sensor (RFS), has a sensing probe that replaces a short length of a refiner bar, enabling measurement of forces normal to and tangential to the refiner bars. The RFS has been used in a number of studies in both low consistency [15,16] and high consistency refining [17,18]. In a recent study, Harirforoush et al. [19] investigated the relation between net power, gap, and forces on bars in LC refining using the RFS. They found that, as the plate gap is reduced, the length-weighted fiber length remains relatively constant while net refiner power and the mean peak normal and shear forces increase up to threshold values. Here, peak refers to the maximum value that occurs as a bar on the rotor passes over the sensor. Above these thresholds, the mean peak normal and shear forces continue to increase, but the length-weighted fiber length exhibits negative linear relationship with these forces.

The objective of this study is to investigate the onset of fiber cutting based on analysis of bar forces measured with the RFS at a wide range of rotational speeds at 2.5% and 3.5% consistency. Distributions of the peak normal and shear forces, and peak coefficient of friction (i.e., peak shear force divide by peak normal force) are determined for each operating condition. Distinct transitions occur in these distributions that correspond to the onset of fiber cutting. In addition, frequency analysis of the sensor data shows that the magnitude of the dominant frequency can be used as an indication of the onset of fiber cutting.

MATERIALS AND METHODS

Trials were conducted using the AIKAWA 16-in. single-disc refiner at the Pulp and Paper Center at the University of British Columbia (Vancouver, BC, Canada). The refiner is equipped with a power meter, plate actuation, and a variable speed drive. The plate used in these trials is manufactured by AIKAWA FINEBAR, which has bar edge length of 2.74 km/rev and bar angle of 15° from radial. The bar width, groove width, and groove depth of the plate are 1.6 mm, 3.2 mm, and 4.8 mm, respectively.

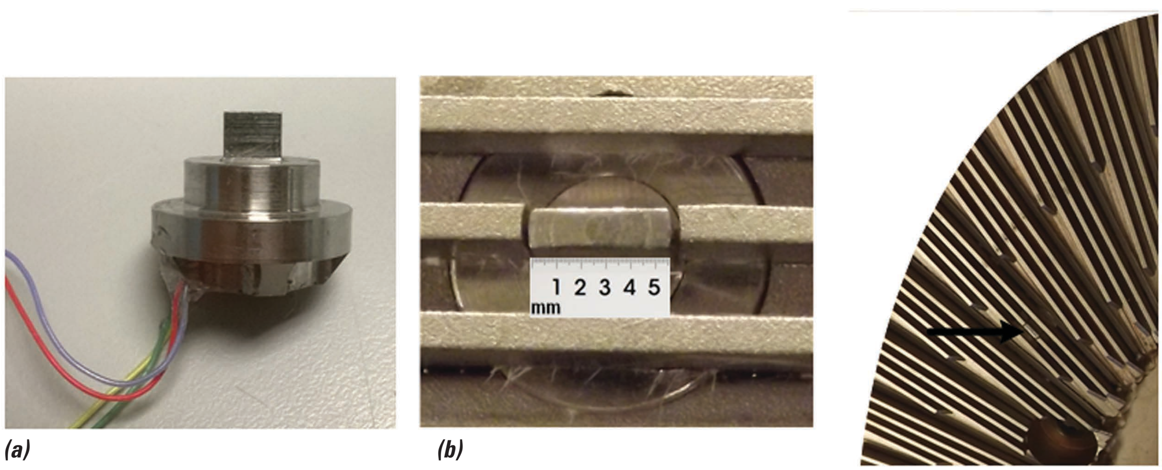

(a) (b) (c)

1. (a) Refiner force sensor (RFS) used at the Pulp and Paper Center, University of British Columbia (Vancouver, BC, Canada) trials, (b) a close-up of RFS installed in the stator plate, and (c) the location of the sensor in the stator plate [19].

An RFS-type sensor was custom designed and fabricated based on the design previously used in refiner trials [20]. A photograph of the RFS used in this work is shown in **Fig. 1a**. The sensor is installed in a custom recess that is machined into the back of the stator plate. The sensor wires pass from the back side of the sensor and through a custom gland located in the door of the refiner. The sensor recess is located so that the tip of the sensor replaces a short length of the refiner bar (i.e., 5 mm), as shown in Fig. 1b. The sensor measures force normal to the plate surface (i.e., parallel to the axis of the refiner bar) and the shear force perpendicular to the major axis of the refiner bar and normal to the bar edge. The sensor is positioned in the second bar of a three-bar cluster at a radius of 151 mm, as shown in Fig 1c. At this radius, the heads of the bolts do not pass over the sensor. The 144 bars on the rotor, grouped into 48 three-bar clusters, cross over the sensor in one revolution of the refiner.

Calibration and environmental tests were performed as described in [19,21]. Modal analyses were performed to ensure that the first natural frequency of the sensor is well above the bar-passing frequency of the refiner so that phase and magnitude distortion due to sensor resonance is avoided. The ratio of the first natural frequency of the sensor to the maximum bar-passing frequency is 8.2, which provides a sufficient margin above the bar passing frequency.

A custom charge amplifier converts the high impedance charge output of the sensors to a low impedance voltage signal that is read by a National Instruments (Austin, TX, USA) PXI 1042 Q high-speed board. National Instrument BNC-2110, Shielded Connector Blocks are used to connect the high-speed DAQ board to the charge amplifier. A custom LabVIEW (National Instruments; Austin, TX, USA) interface is used to control data acquisition. A sampling rate of 150 kHz is used, which is more than twenty times the maximum bar-passing frequency that occurs during the trials.

Mechanical SPF (40% spruce; 45% pine; 10% balsam fir and 5% Douglas fir) softwood pulp, produced at Quesnel River Pulp Mill, with 378 ml CSF at 2.5% and 3.5% consistency was used in all trials. The operating conditions for the trials are shown in **Table I**. The refining operating mode was mono-flo with one inlet perpendicular to the outlet. The refiner speed was set with a variable frequency drive (VFD). The plate gaps were adjusted using a controller from no-load position (3.5 mm) to the smaller plate gaps (0.25 mm). The flow rate was held constant at 250 L/min. Sensor signals were recorded using the LabVIEW interface for approximately 10 s once reaching stable condition at each target point. At each operating condition, the refiner was held steady for about 10 s to give the pulp time to move from the refining zone to the sample collection point. A 2-L pulp sample was collected over a 5 s interval. The process was repeated until all of the target points were achieved for one rotational speed. Then, the plate gap was increased to the no-load position and the refiner was adjusted to the next rotational speed using the VFD.

The length-weighted fiber length (L_W) was measured for all pulp samples using a Fiber Quality Analyzer (HiRes FQA, Optest Equipment Inc.; Hawkesbury, ON, Canada). Length-weighted fiber length is calculated based on Eq. (1) [22]:

$$L_w = \frac{\sum n_i L_i^2}{\sum n_i L_i} \tag{1}$$

where, n_i and L_i are the number of the fibers in the ith class and mean length of the ith class, respectively.

An algorithm was created in MATLAB (Mathworks; Natick, MA, USA) to identify bar-passing events in the force data. A bar-passing event is defined to occur when the passage of a rotor bar over the sensor results in a maximum or peak value in the force data that exceeds a predefined threshold value. The algorithm and its verification are described in [19].

For each bar-passing event, peak force is defined as the difference between the force at the base of the local valley that precedes the peak and the force at the peak [16]. The peak coefficient of friction is calculated by dividing the peak shear force by the peak normal force. The peak force and peak coefficient of friction data are assessed in the form of distributions to which the two-parameter Weibull distribution function is fit.

The Weibull distribution function is widely used because of its ability to characterize a wide variety of distributions, and

Parameter	Condition	
Refiner speed, rpm	800, 1000, 1200	1200
Consistency	3.5 %	2.5 %
Flow rate, L/min	250	
Plate gap, mm	3.5–0.25 (15 gaps)	3.5–0.25 (12 gaps)
Operating mode	Mono-flo	
Pulp type	Mechanical SPF softwood pulp, starting freeness at 378 ml CSF	

I. Operating conditions for the pilot-scale low consistency refining trials at the Pulp and Paper Center, University of British Columbia.

it has been used in previous HC and LC refining studies [15,17]. The Weibull distribution function is shown in Eq. (2) [23]:

$$f(x) = \frac{\beta}{\eta}\left(\frac{x-\gamma}{\eta}\right)^{\beta-1} exp^{-\left(\frac{x-\gamma}{\eta}\right)^{\beta}} \quad (2)$$

where, β, η, and γ are shape, scale and location parameters, respectively. The effects of these parameters on the Weibull distribution are discussed by Lee [24]. The two-parameter Weibull distribution function is obtained by setting in Eq. (2). In this study, the Weibull scale and shape parameters of the peak normal, shear force, and peak coefficient of friction distributions are calculated for each operating condition. Each of these parameters are then correlated to both plate gap and L_W.

RESULTS

The relation between net power and the inverse of plate gap for three rotational speeds (i.e., 1200 rpm, 1000 rpm, and 800 rpm) at 3.5% consistency and 1200 rpm at 2.5% consistency is shown in **Fig. 2**. In all cases, the net power increases as the plate gap is reduced. However, a considerable increase in energy transferred to the fibers is seen for gaps of less than 0.5 mm (or more than 2 mm^{-1}). At a constant gap and consistency, increasing the rotational speed increases the net power. The relationships are similar to the results of Nugroho [10], Elahimehr et al. [11], and Harirforoush et al. [19]. Across the full range of gaps at 1200 rpm, the net power for 3.5% and 2.5% consistency are approximately equal.

The relation between L_W and the inverse of plate gap for three rotational speeds (i.e., 1200 rpm, 1000 rpm, and 800 rpm) at 3.5% consistency and 1200 rpm at 2.5% consistency is shown in **Fig. 3**. In each case, L_W remains relatively constant as the plate gap is closed until the gap reaches the critical value, indicated by the dashed lines. The critical values are determined based on transitions in the plot of L_W versus the inverse of plate gap. For plate gaps smaller than the critical gap, L_W decreases in an approximately linear manner.

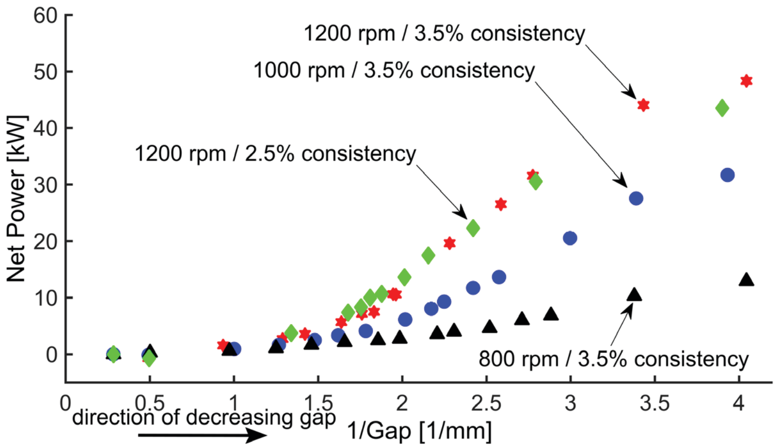

2. Net power versus the inverse of plate gap for three rotational speeds (i.e., 1200 rpm, 1000 rpm, and 800 rpm) at 3.5% consistency. Data is also shown for 1200 rpm at 2.5% consistency.

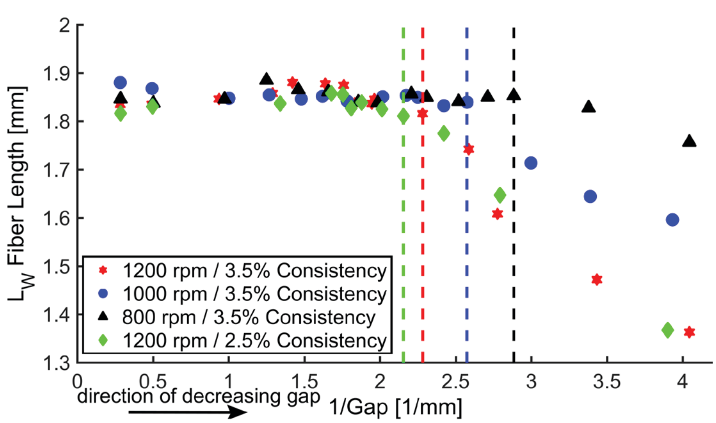

3. L_W versus the inverse of plate gap for three rotational speeds (i.e., 1200 rpm, 1000 rpm, and 800 rpm) at 3.5% consistency. Data is also shown for 1200 rpm at 2.5% consistency.

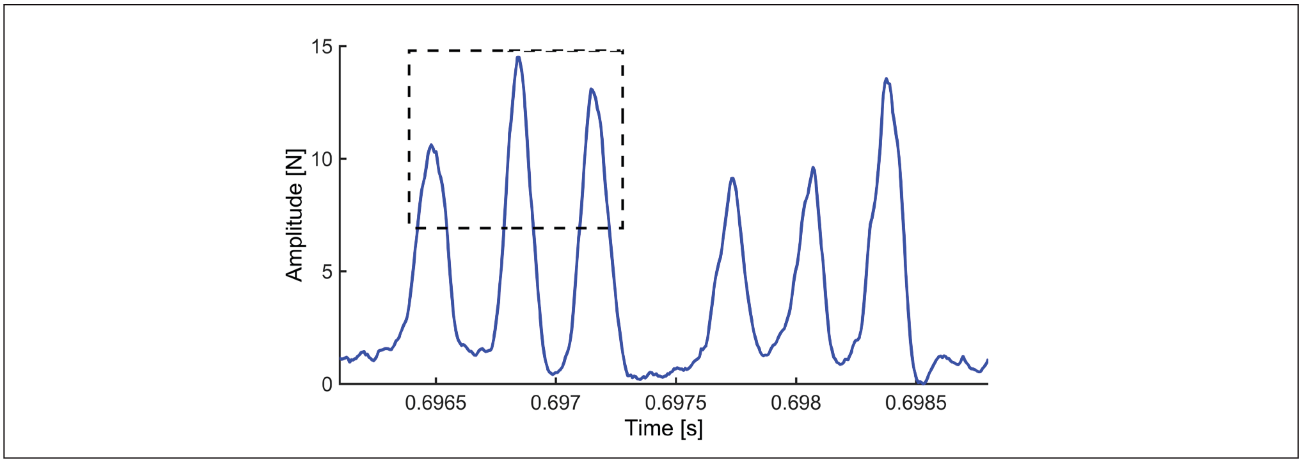

4. Typical unfiltered normal force data at 1000 rpm and 0.45 mm plate gap.

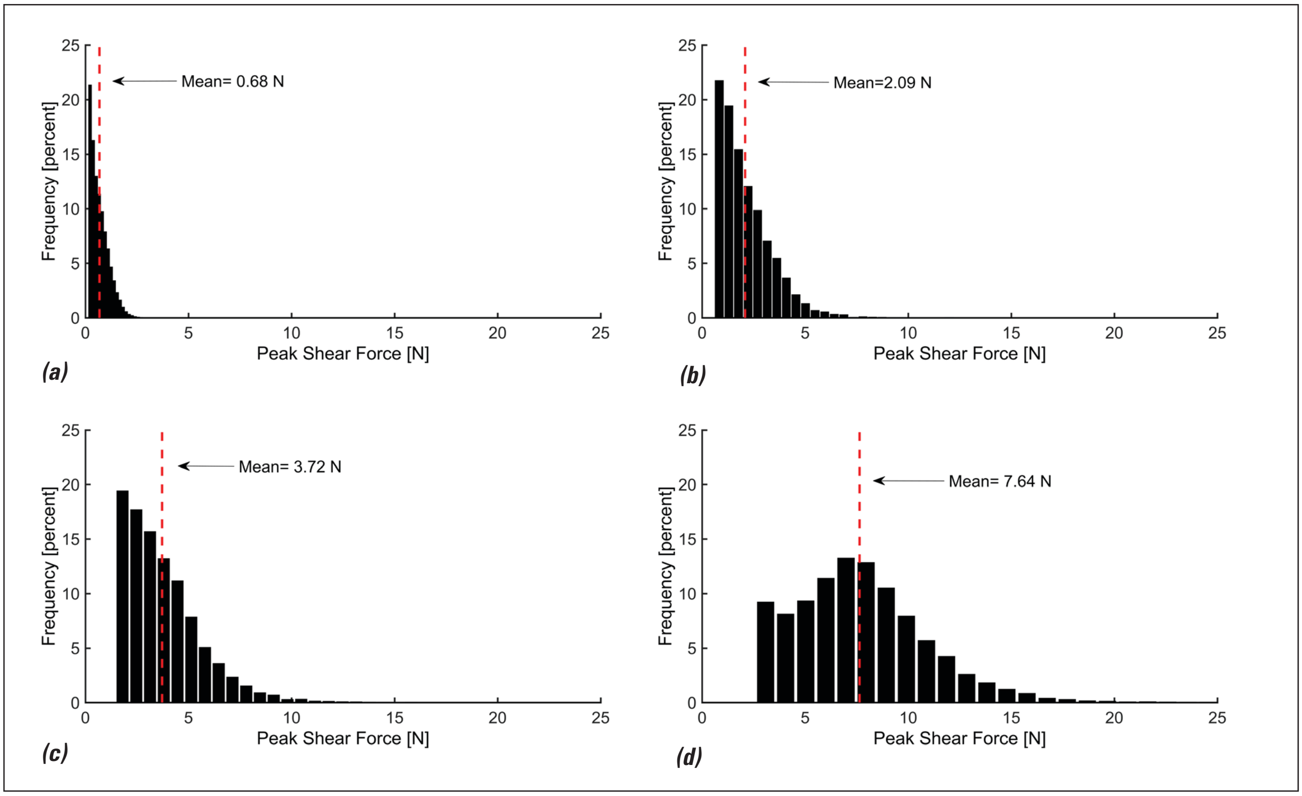

5. Normalized distributions of peak shear force for plate gaps of (a) 3.5 mm, (b) 0.55 mm, (c) 0.4 mm, and (d) 0.3 mm for rotational speed of 1200 rpm at 3.5% consistency.

Figure 3 also shows that, at the same consistency (i.e., 3.5%), the critical gap decreases as rotational speed decreases. This finding is consistent with the results of Nugroho [10], Elahimehr et al. [11], and Harirforoush et al. [19]. Moreover, the red dashed line representing the critical gap for 1200 rpm at 3.5% consistency occurs where 1/Gap = 2.282 (or gap = 0.438 mm), while the green dashed line indicating the critical gap for 1200 rpm at 2.5% consistency occurs where 1/Gap = 2.155 (or gap = 0.464 mm). Thus, at the same rotational speed, decreasing the consistency from 3.5% to 2.5% slightly increases the critical gap. This trend is not in agreement with Lundin [25], who reported that decreasing the consistency from 6% to 3% decreases the critical gap from 0.27 mm to 0.2 mm.

Typical unfiltered normal force data, taken at 1000 rpm and a plate gap of 0.45 mm, is shown in **Fig. 4**. Each peak represents a bar-passing event. As highlighted by the dashed rectangle, bar-passing events appear as clusters of three peaks, since the bars of the rotor that cross over the force sensor are grouped in three-bar clusters.

Normalized distributions of peak shear force data for plate gaps of 3.5 mm (no-load), 0.55 mm, 0.4 mm, and 0.3 mm for 1200 rpm at 3.5% consistency are shown in **Fig. 5**. The mean

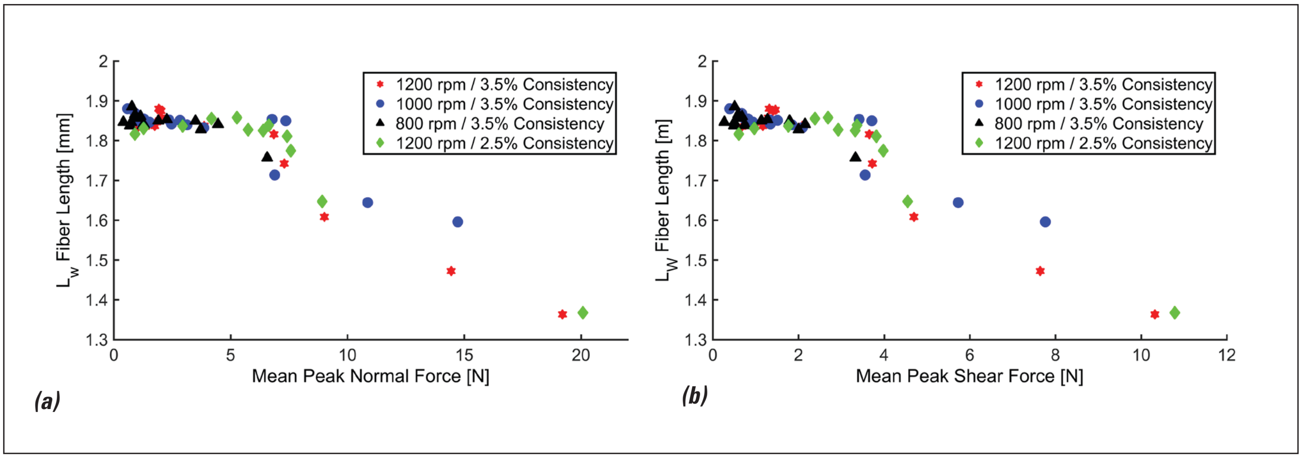

6. (a) L_w versus mean peak normal and (b) shear force for three rotational speeds (i.e., 1200 rpm, 1000 rpm, and 800 rpm) at 3.5% consistency. Data is also shown for 1200 rpm at 2.5% consistency.

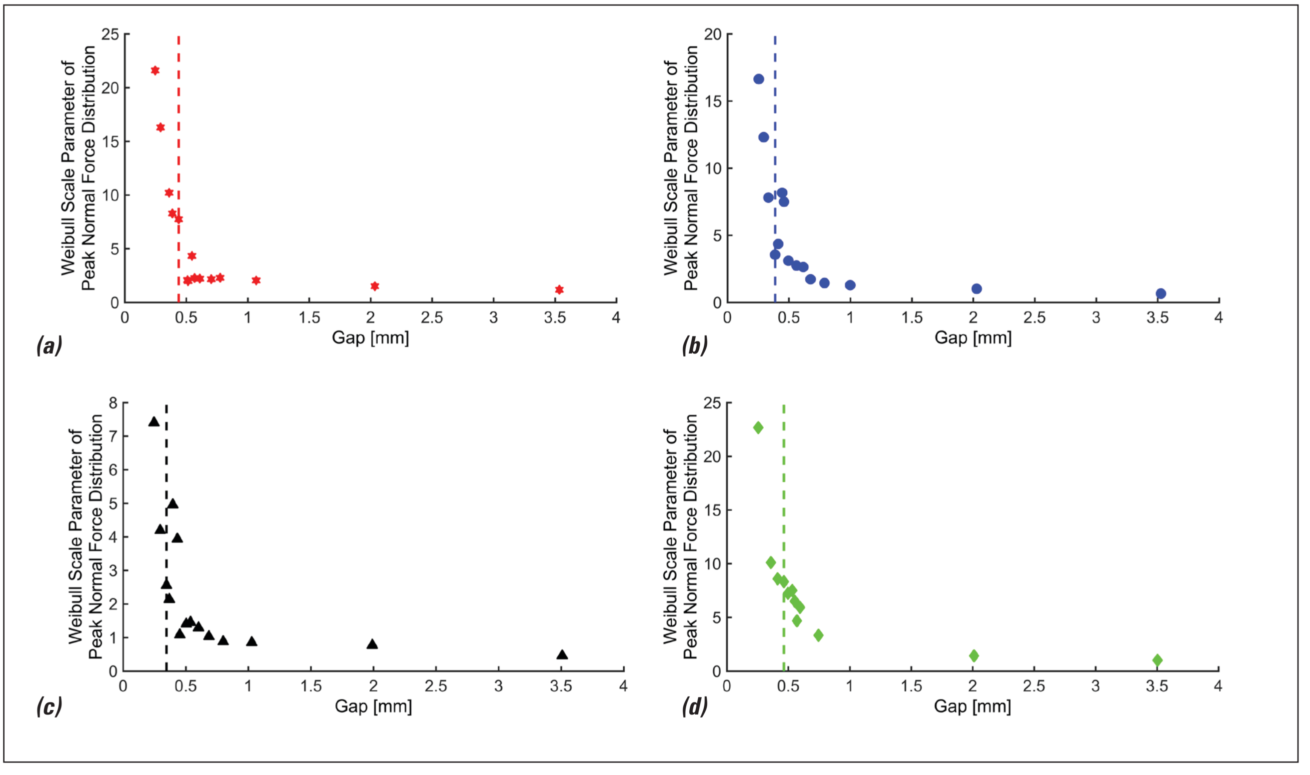

7. The Weibull scale parameter of peak normal force distribution versus plate gap for rotational speeds of (a) 1200 rpm, (b) 1000 rpm, (c) 800 rpm at 3.5% consistency, and (d) 1200 rpm at 2.5% consistency.

value of the peak shear force distribution, highlighted by the dashed line, increases as the plate gap decreases, which is consistent with the increase in net refiner power. This result is in agreement with the results of Prairie et al. [15], who showed that the median forces increase with increasing specific edge load (SEL). Moreover, as the plate gap is closed, the distribution of peak shear forces is extended to the right, its height decreases, and the shape of the distribution changes from positively skewed to an approximately normal distribution. The truncation of the left-hand end of the distributions shown in Figs. 5b, 5c, and 5d is an artefact of the algorithm used to identify bar-passing events. This algorithm, which is described in [19], discards events that fall below a prescribed threshold.

Figure 6 shows the relationship between L_W and mean peak force for three rotational speeds (i.e., 1200 rpm, 1000 rpm, and 800 rpm) at 3.5% consistency and 1200 rpm at 2.5% consistency. As shown in Fig. 6a, L_W remains relatively unchanged as mean peak normal force increases up to a threshold value that corresponds to the critical gap. The L_W value decreases in an approximately linear manner beyond the critical gap threshold. The trend is consistent with the results of Harirforoush et al. [19]. The mean peak normal force at this

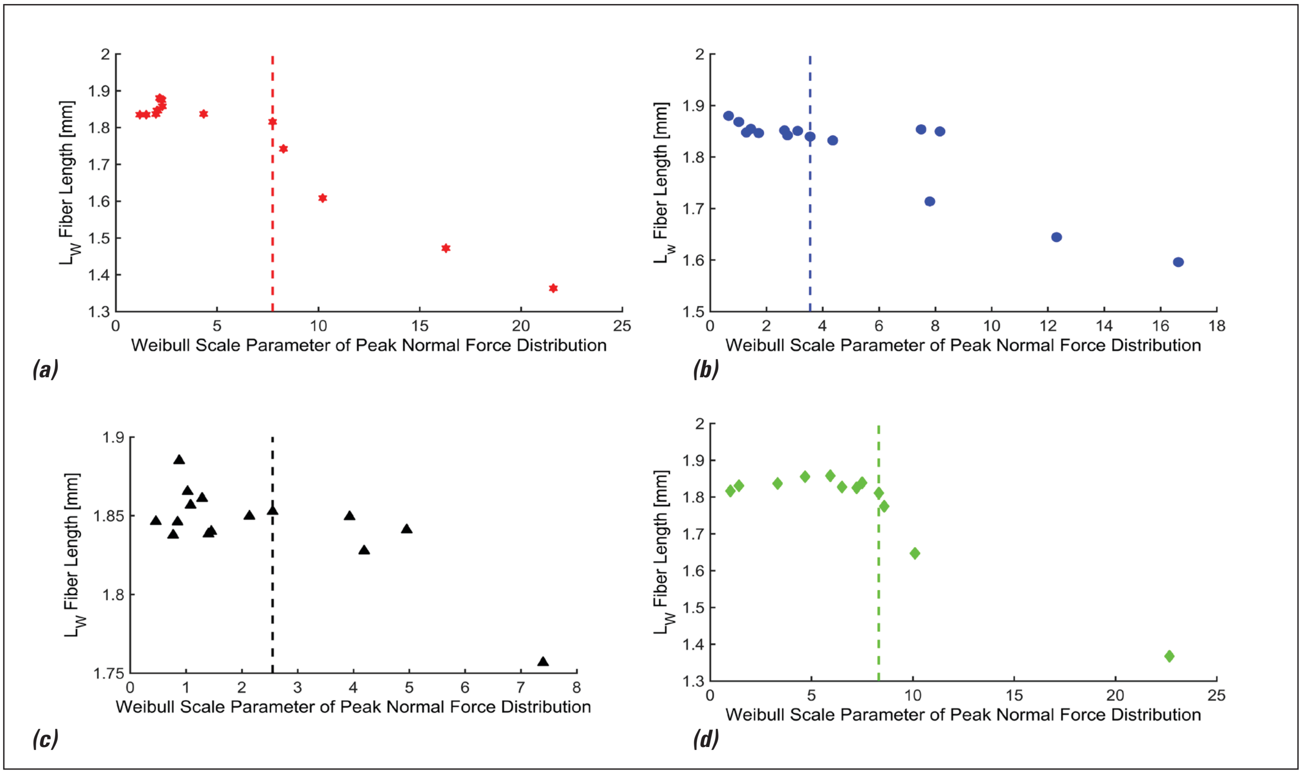

8. L_w ***versus the Weibull scale parameter of peak normal force distribution for rotational speeds of (a) 1200 rpm, (b) 1000 rpm, (c) 800 rpm at 3.5% consistency, and (d) 1200 rpm at 2.5% consistency.***

threshold is relatively constant, approximately 7 N, for all rotational speeds at 3.5% consistency. Decreasing the consistency from 3.5% to 2.5% slightly increases this threshold value.

A similar trend is seen in the relationship between L_W and mean peak shear force (Fig. 6b). However, the threshold value at which the transition occurs is lower, approximately 3.8 N. For 800 rpm, possibly due to insufficient data for the plate gaps less than the critical gap, the trend cannot be seen.

To explore the relationship between the distribution of peak force and plate gap, the Weibull scale parameter of peak normal force distribution is plotted versus plate gap for three rotational speeds (i.e., 1200 rpm, 1000 rpm, and 800 rpm) at 3.5% consistency and 1200 rpm at 2.5% consistency. As shown in **Fig. 7a**, as the plate gap is decreased, the scale parameter remains relatively constant up to a threshold value. The threshold, highlighted by dashed line, corresponds to the transition seen in the plot of L_W versus the inverse of plate gap for 1200 rpm at 3.5% consistency, Fig. 3. This transition is in agreement with the onset of the fiber cutting. The trend also appears in Figs. 7b, 7c and 7d but is less definitive for 800 rpm at 3.5% consistency, Fig. 7c, and 1200 rpm at 2.5% consistency, Fig. 7d.

The relation between the distribution of peak forces and fiber length is investigated by plotting L_W versus the Weibull scale parameter of peak normal force distribution for three rotational speeds (i.e., 1200 rpm, 1000 rpm, and 800 rpm) at 3.5% consistency and 1200 rpm at 2.5% consistency. As shown in **Fig. 8a**, the length-weighted fiber length remains relatively constant as the scale parameter increases up to a threshold value, highlighted by dashed line. The dashed line corresponds to the transition seen in the plot of L_W versus the inverse of plate gap, Fig. 3, and it is at the same position as the dashed line shown in Fig. 7a. The L_W value decreases beyond this point. This point corresponds to the onset of fiber cutting. Similar trends occur in Figs. 8b, 8c, and 8d but are less definitive for 1000 rpm, Fig. 8b, and 800 rpm, Fig. 8c. At 800 rpm, pulp flow rate was observed to be unstable which may reflect unstable conditions in the refiner and may also be the cause of anomalous data at this speed.

The mean coefficient of friction is plotted in **Fig. 9a** as a function of SEL for three rotational speeds (i.e., 1200 rpm, 1000 rpm, and 800 rpm) at 3.5% consistency and for 1200 rpm at 2.5% consistency. Mean coefficient of friction decreases with increasing SEL. This result is consistent with Prairie et al. [15]. As shown in Fig. 9b, the mean coefficient of friction decreases as the plate gap is reduced. This finding is in accordance with Senger et al. [26]. The mean coefficient of friction varies from 0.65 to 1.37.

The relationships between L_W and the Weibull scale parameter of the distribution of peak coefficient of friction for three rotational speeds (i.e., 1200 rpm, 1000 rpm, and 800 rpm) at 3.5% consistency and 1200 rpm at 2.5% consistency are shown in **Figs. 10a-10d**. As shown in Fig. 10a, L_W remains relatively constant as the scale parameter decreases to a threshold, highlighted by a dashed line. The dashed line is at the same point as the dashed lines shown in Fig. 7a and Fig 8a, and it is

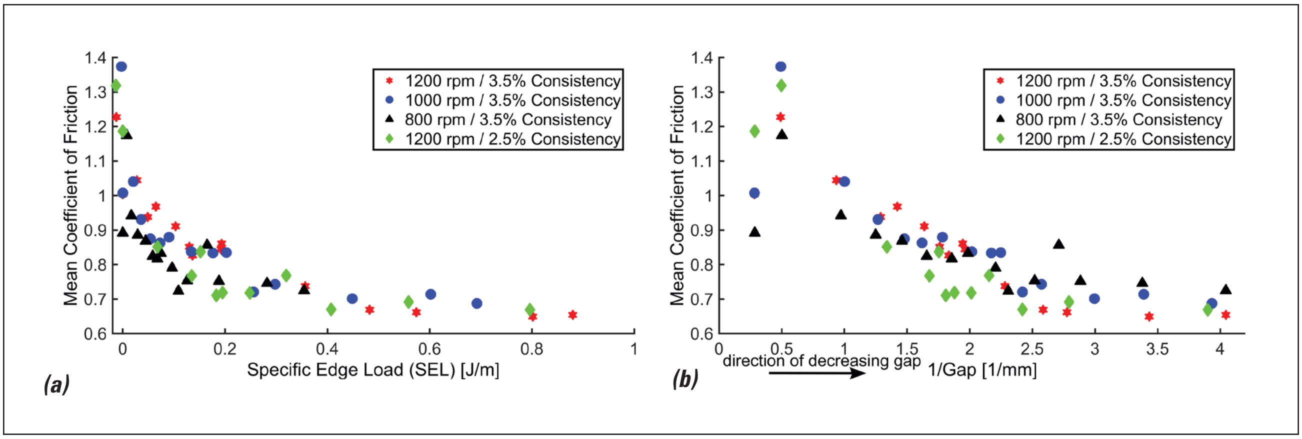

9. (a) Mean coefficient of friction versus specific edge load (SEL), and (b) mean coefficient of friction versus plate gap for three rotational speeds (i.e., 1200 rpm, 1000 rpm, and 800 rpm) at 3.5% consistency. Data is also shown for 1200 rpm at 2.5% consistency.

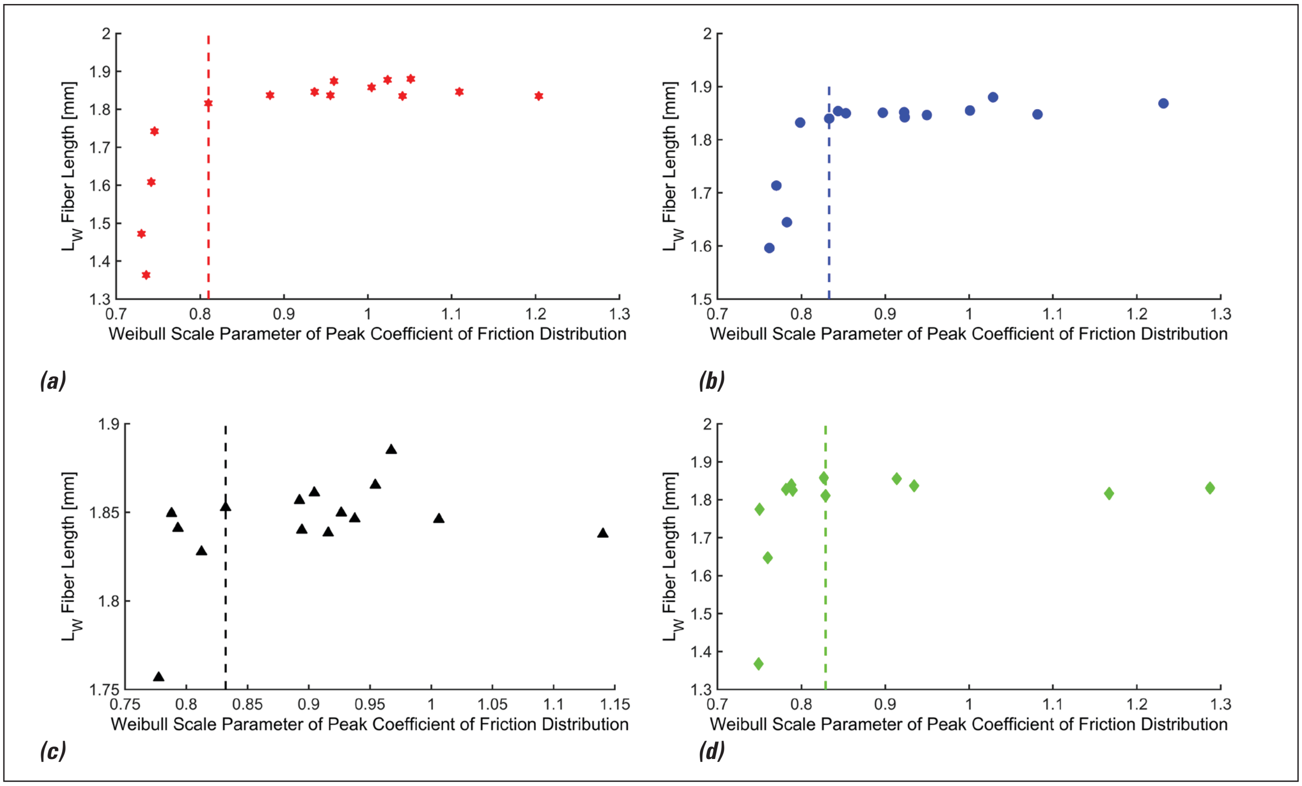

10. L_w versus Weibull scale parameter of peak coefficient of friction distribution for rotational speeds of (a) 1200 rpm, (b) 1000 rpm, (c) 800 rpm at 3.5% consistency, and (d) 1200 rpm at 2.5% consistency.

determined based on the transition seen in the plot of L_W versus the inverse of plate gap, Fig. 3. This point corresponds to the onset of fiber cutting. The L_W value decreases beyond this point. Similar transitions occur in Figs. 10b, 10c, and 10d.

The spectra of the normal force data at 1200 rpm, plate gaps of 0.45 mm and 0.55 mm, and 3.5% consistency show four maxima at frequencies of 3.82, 2.87, 1.90, and 0.95 kHz, highlighted by dashed circles, **Fig. 11**. The frequencies correspond to crossings of different bars within the three-bar clusters of the rotor, as described in [19]. The highest amplitude, marked by the arrow, corresponds to the passage of equivalent edges in adjacent three-bar clusters. This frequency, referred to here as the dominant frequency ($Freq_d$), appears in the frequency analysis for all of the operating conditions. Comparing Fig. 11a and Fig. 11b, it is apparent that the amplitude (magnitude) at this frequency is affected by the plate gap.

Figure 12 shows the magnitude of the dominant frequency, ($Freq_d$), versus plate gap for three rotational speeds (i.e., 1200 rpm, 1000 rpm, and 800 rpm) at 3.5% consistency and 1200 rpm at 2.5% consistency for normal force data. As shown in Fig. 12a, the magnitude remains relatively constant while the plate gap is reduced up to a threshold value, which

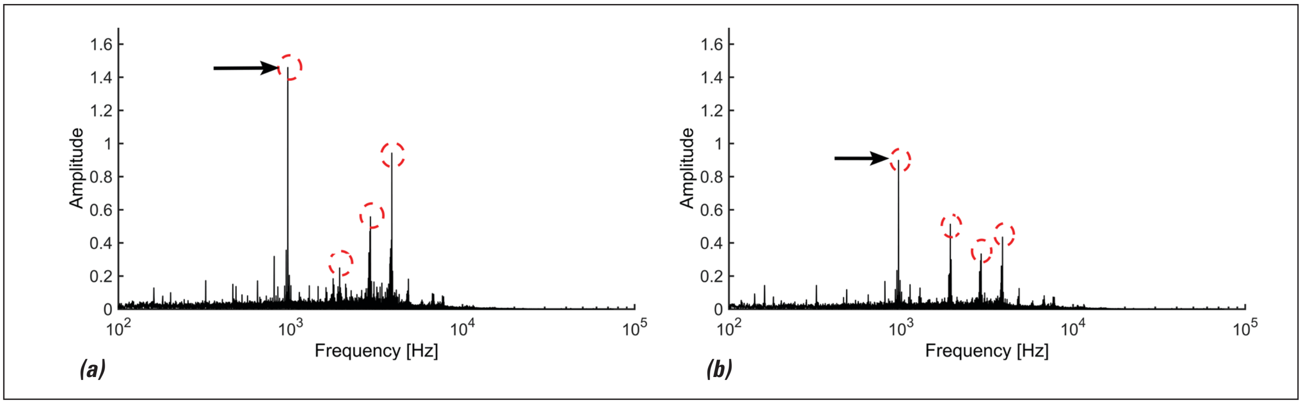

11. Spectrum of normal forces at plate gaps of (a) 0.45 mm and (b) 0.55 mm for rotational speed of 1200 rpm and 3.5% consistency.

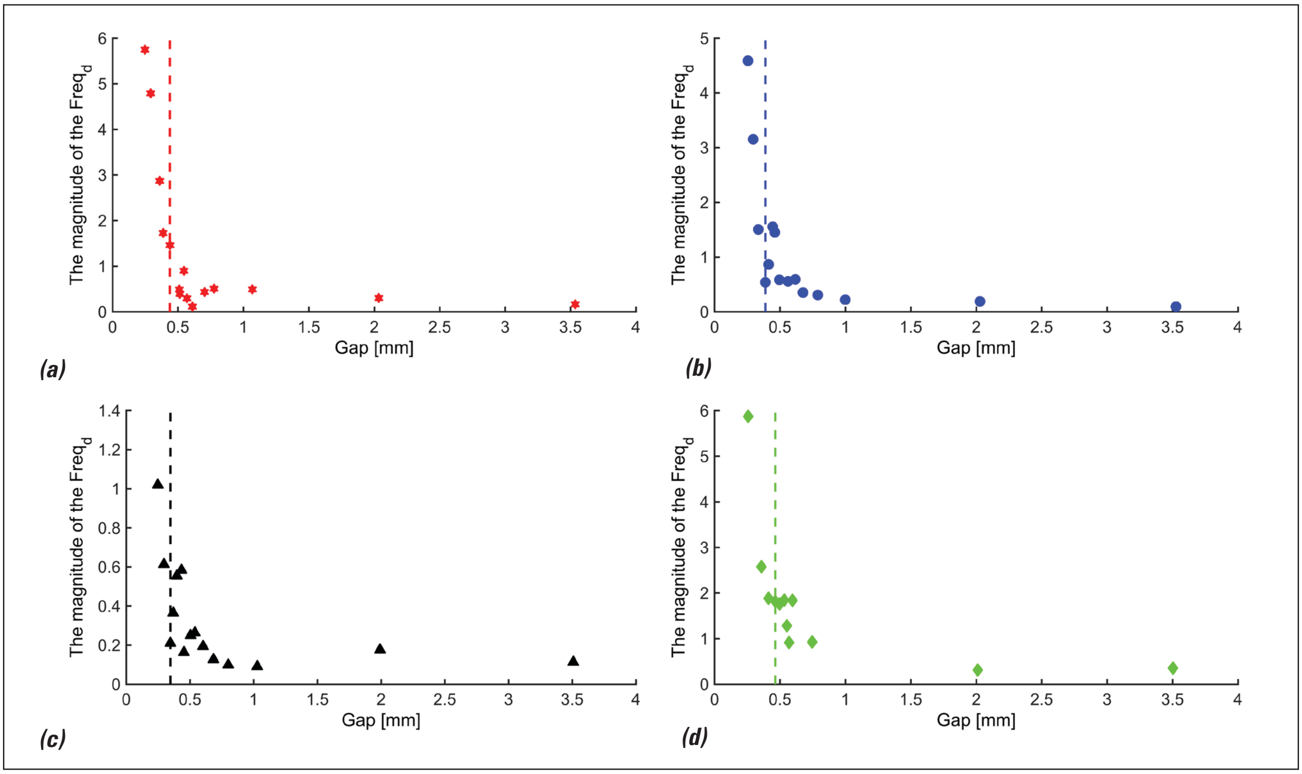

12. The magnitude of the frequency corresponds to the passage of equivalent edges in adjacent three-bar clusters versus the plate gap for rotational speeds of (a) 1200 rpm, (b) 1000 rpm, (c) 800 rpm at 3.5% consistency, and (d) 1200 rpm at 2.5% consistency.

corresponds to the onset of fiber cutting, indicated by dashed lines. This trend is present but less definitive for 800 rpm, Fig. 12c, and 1200 rpm at 2.5% consistency, Fig. 12d.

The trends shown in Figs. 7, 8, and 12 also appear in the peak shear force distributions. This data is not included here in the interest of brevity.

DISCUSSION

The RFS measures normal force and shear force, perpendicular to the major axis of the refiner bar, in a single-disc LC refiner. The bar-passing events are characterized as distributions of event parameters such as peak normal and shear forces and peak coefficient of friction. These distributions are used to compare refining conditions on the basis of data taken at each operating condition. Distinct transitions are observed in parameters that characterize these distributions; in particular, mean peak force and the Weibull scale parameter. These transitions consistently correspond to the onset of fiber cutting.

As the plate gap is reduced, mean peak normal and shear forces increase but L_W remains relatively constant, up to a threshold value of mean peak normal and shear force. The L_W value decreases in an approximately linear manner beyond these threshold values, as shown in Fig. 6. These transitions correspond to the onset of fiber cutting. Above these thresholds, mean peak forces continue to increase but L_W exhibits a negative linear relationship with force that mirrors the established relationship between L_W and the inverse of plate gap (Fig. 3). The trend is consistent with the results in [19].

The Weibull scale parameter of the peak force distributions and of peak coefficient of friction distributions are also candidates for in-process detection of fiber cutting. As shown in Fig. 8 and Fig. 10, transitions occur in length-weighted fiber length at the values of the scale parameters that correspond to the onset of fiber cutting. Note that the position of these transitions, indicated by the dashed lines, correspond to the transitions seen in the plot of L_W versus the inverse of plate gap shown in Fig. 3.

In addition to these indicators of fiber cutting found in the time domain data, the power spectrum of the sensor data can also be used to detect the onset of fiber cutting. As shown in Fig. 12, as the plate gap is reduced, the magnitude of the dominant frequency, which is equal to the bar-passing frequency, remains relatively constant up to a threshold value that corresponds to the onset of fiber cutting. Beyond this threshold, the amplitude increases. According to Parseval's theorem, the magnitude of the spectrum at a given frequency is equal to the energy transferred at that frequency. Therefore, this transition in the spectrum may be due to a fundamental change in the mode of energy transfer to the pulp at the onset of fiber cutting.

These results suggest that the RFS has potential to be used for in-process detection of fiber cutting in mill operations. In previous mill trials, the sensors have been shown to be sufficiently rugged [17] for industrial use. Key challenges to such an application are modification of refiner plates to accommodate the sensors and passage of signal wires from the sensor to the refiner exterior.

CONCLUSION

This study investigates in-process detection of the onset of fiber cutting using a custom designed piezoelectric sensor measuring normal and shear forces, perpendicular to the major axis of the refiner bars, in an AIKAWA/Advanced Fiber Technologies Inc. 16-in. single-disc LC refiner. Trials were run using mechanical SPF softwood pulp with 378 ml CSF at 2.5% and 3.5% consistency for three rotational speeds (1200, 1000, and 800 rpm) and a wide range of plate gaps. The pulp was sampled at regular intervals, and the length-weighted fiber length was determined for each sample. The data recorded from the sensors were processed and the distributions of the peak normal and shear forces and peak coefficient of friction are determined for each operating condition. A two-parameter Weibull function is fit to each of these distributions. The Weibull scale parameter is calculated and length-weighted fiber length is plotted as a function of this parameter. The results show that the onset of fiber cutting consistently corresponds to a distinct transition in the plot of length-weighted fiber length versus scale parameter. In addition, the power spectrum of the sensor data indicates that the magnitude of the dominant frequency can be used as an indication of the onset of fiber cutting. This result suggests that the sensor has potential to be used for in-process detection of the onset of fiber cutting. **TJ**

ACKNOWLEDGEMENTS

This work is funded by a Collaborative Research and Development grant provided by National Sciences and Engineering Research Council of Canada (NSERC) and the following partners, who we thank for their ongoing support: AB Enzymes, Alberta Newsprint Company, Andritz, BC Hydro, Canfor, Catalyst Paper, FPInnovations, Holmen Paper, Meadow Lake Pulp (Paper Excellence), Millar Western, NORPAC, West Fraser, Westcan Engineering, and Winstone Pulp International.

A special thanks to M. Miller, E. Jahangir, E. Trudel, G. Burton, and G. Soong for their assistance during the preparation and execution of the refining trials at the Pulp and Paper Center at the University of British Columbia.

LITERATURE CITED

1. Luukkonen, A., Olson, J.A., and Martinez, D.M., *J. Pulp Pap. Sci.* 36(1-2): 28(2010).
2. Muenster H., Ferritsius O., Lecourt M., et al., *Proc. Int. Mech. Pulping Conf.*, TAPPI Press, Atlanta, GA, USA, 2005, p. 213.
3. Zha, Q., Lanouette, R., Law, K.-N., et al., *Prepr. - PAPTAC Annu. Meet., 94th*, Pulp and Paper Technical Association of Canada, Montreal, 2008, p. B481.
4. Musselman, R., Letarte, D., and Simard, R., *Int. Refin. Conf., 4th*, Pira International, Leatherhead, UK, 1997, pp.139–148.
5. Sandberg., C., Sundström, L., and Nilsson, L., *Proc. Int. Mech. Pulping Conf.*, TAPPI Press, Atlanta, 2009, p. 186.
6. Kappel, J., *Mechanical Pulps: From Wood to Bleached Pulp*, TAPPI Press, Atlanta, 1999.
7. Smook, G.A., *Handbook for Pulp and Paper Technologists*, 2nd Edn., Angus Wilde Publications, Vanouver, BC, Canada, 1992.
8. Luukkonen, A., Olson, J.A., and Martinez, D.M., *J. Pulp Pap. Sci.*, 36(3-4): 107(2010).
9. Luukkonen, A., Ph.D. thesis, "Development of a methodology to optimize low consistency refining of mechanical pulp," University of British Columbia, Vancouver, 2011.
10. Nugroho, D.D.P., "Low consistency refining of mixtures of softwood and hardwood bleached kraft pulp: Effects of refining power," M.Sc. thesis, Asian Institute of Technology, Khlong Nung, Thailand, 2012.
11. Elahimehr, A., Olson, J.A., and Martinez, D.M., *Nord. Pulp Pap. Res. J.* 28(3): 386(2013).
12. Berg, J.E., Sandberg, C., Engberg, B., et al., *Nord. Pulp. Pap. Res. J.* 30(2): 225(2015).
13. Kerekes, R.J. and Senger, J.J., *J. Pulp Pap. Sci*. 32(1): 1(2006).
14. Kerekes, R.J., *Nord. Pulp Pap. Res. J.* 26(1): 14(2011).
15. Prairie, B., Wild, P., Byrnes, P., et al., *J. Pulp Pap. Sci.* 34(1): 1(2008).
16. Prairie, B., Wild, P., Byrnes, P., et al., *J. Pulp Pap. Sci.* 108(9): 34(2007).
17. Olender, D., Wild, P., Byrnes, P., et al., *J. Pulp Pap. Sci.* 33(3): 163(2007).

18. Olender, D., Wild, P., Byrnes, P., et al., *Nord. Pulp Pap. Res. J.* 23(2): 218(2008).
19. Harirforoush, R., Wild, P., and Olson, J., *Nord. Pulp Pap. Res. J.* 31(1): 71(2016).
20. Olender, D., Wild, P., and Byrnes P., *J. Process Mech. Eng.* 222(Part E): 115(2008).
21. Prairie, B.C., "Measurement of forces in a low consistency refiner," M.Sc. thesis, University of Victoria, Victoria, BC, Canada, 2005.
22. Graca Carvalho, M., Ferriera, P.J., Martins, A.A., et al., *TAPPI J.* 80(2): 137(1997).
23. Prabhakar Murthy, D.N., Xie, M., and Jiang, R., *Weibull Models*, John Wiley & Sons, Hoboken, NJ, USA, 2003.
24. Lee, S., *Int. J. Basic Appl. Sci.* 14(2): 18(2014).
25. Lundin, T., Ph.D. thesis, "Tailoring pulp fibre properties in low consistency refining," Laboratory of Fiber and Cellulose Technology, Abo Akademyi University, Turku, Finland, 2008.
26. Senger, J., Siadat, A., Ouellet, D., et al., *J. Pulp Pap. Sci.* 30(9): 247(2004).

ABOUT THE AUTHORS

Low consistency (LC) refining of mechanical pulp has been shown to be more energy efficient than conventional high consistency refining. However, degradation of mechanical properties due to fiber cutting at high refining energies has limited the widespread adoption of LC refining. In-process detection of the onset of fiber cutting is essential to reduce fiber cutting.

In 2016, we investigated relationships between local bar forces, plate gap, and fiber length in a single-disc low consistency refiner (Harirforoush et al. [19]). The results showed that the sensors have potential for the onset detection of fiber cutting.

Developing the sensor to withstand the harsh conditions inside the refiner was the most difficult aspect of the research here. Our results suggest that these sensors have potential to be used for in-process detection of the onset of fiber cutting.

The most interesting findings we observed were the distinct transitions in parameters that characterize the distributions of bar forces (forces applied to pulp fibers by the refiner bars). These transitions consistently correspond to the onset of fiber cutting. In addition, the power spectrum of the sensor data indicates that the magnitude of the dominant frequency can be used as an indication of the onset of fiber cutting.

For mills, detection of the onset of fiber cutting

Harirforoush

Wild

Olson

conditions is potentially beneficial in low consistency refining as it may reduce fiber cutting, optimize fiber quality improvements, and increase energy efficiency. Our next step is to understand the effect of pulp furnish on the distribution of bar forces and investigate the onset of fiber cutting by using the sensor data.

Harirforoush is a Ph.D. candidate in the Department of Mechanical Engineering and the Institute for Integrated Energy Systems (IESVic), and Wild is professor of Mechanical Engineering and director of IESVic, at the University of Victoria, Victoria, BC, Canada. Olson is associate dean of Research and Industrial Partnership, Faculty of Applied Science; professor of Mechanical Engineering; and FPInnovations professor at the University of British Columbia – Point Grey Campus, Vancouver, BC, Canada. Email Harirforoush at rharirfo@uvic.ca.